Rational drug design and synthesis of some 2-(2-phenyl-1*H*-benzo[*d*]imidazol-1-yl)acetic acid derivatives as potential angiotensin receptor inhibitors

Pravin S. Tajane[1*], Ramesh L. Sawant[2]

[1]Ph. D. Research Scholar, Department of Pharmaceutical Chemistry, Dr. Vithalrao Vikhe Patil Foundation's College of Pharmacy, Ahmednagar (M.S.) India;

[2]Professor, Department of Pharmaceutical Chemistry, Dr. Vithalrao Vikhe Patil Foundation's College of Pharmacy, Ahmednagar (M.S.) India.

***Corresponding Author E-mail:** pravintajane2509@gmail.com*

ABSTRACT:

Background and Objectives: After knowing the importance of benzimidazoles in various diseases, in present work, we aimed at preparing some 2-(2-phenyl-1*H*-benzo[*d*]imidazol-1-yl) acetic acid derivatives as potential angiotensin-II receptor inhibitors. **Method:** The designed derivatives were subjected for the calculations of Lipinski rule, Veber's rule, ADME analysis, drug-likeness properties and molecular docking. The derivatives which successfully passed all the criteria and found potent through *in silico* screening were preceded for the wet lab synthesis, *in vitro*, and *in vivo* biological evaluation. **Results:** From the initial screening through Lipinski rule, Veber's rule, ADME calculations, and drug-likeness properties, molecules A16, A17, A19, A20 and A21 violated the most drug-likeness characteristics. Therefore only remaining molecules were subjected for molecular docking studies. In molecular docking studies we have selected A1, A6, A7, A11, A12, A13, A14, A15 and A18 for the wet lab synthesis and biological evaluation based on their binding affinity with the receptor and formation of hydrogen bonds with crucial amino acids. The synthesized compounds demonstrated good inhibitory potential compared to Captopril although did not exhibited more potency but can be considered active as angiotensin inhibitor. Out of screened derivatives, compounds A1 and A11 showed most potent IC_{50} values of 0.52 and 0.47 µg/mL respectively. From *in vivo* screening compound A11 displayed optimum control on systolic and diastolic BP as well as showed controlled heart rate (beats/min). **Conclusion:** From present study it was concluded that the compounds A1 and A11 have potent angiotensin receptor inhibitory potential and can be treated as potential lead nucleus to generate more potent antihypertensive agents.

Keywords: Benzimidazole; ACE inhibitors; molecular docking, ADMET, *in vitro, in vivo*

DOI Number: 10.14704/nq.2022.20.6.NQ22322 **NeuroQuantology 2022; 20(6) 3184-3200**

1. Introduction

Benzimidazole, also known as 1*H*-benzimidazole and 1,3-benzodiazole, is a significant heterocyclic pharmacophore composed of a benzene ring fused with a five-membered imidazole ring. Heterocyclic chemistry consider benzimidazole to be a "privileged structure" because of the vast variety of biological activities(Alaqeel, 2017; Barot et al., 2013). There were a few theories in the 1940s about benzimidazole's role in biology, and the first study on benzimidazole nucleus' biological activity was published in 1944(Woolley, 1944). When **Brink et al.**(Brink and Folkers, 1949) discovered that 5,6-dimethylbenzimidazole was a breakdown product of vitamin B12 and several of its derivatives also exhibited vitamin B12-like action, interest among researchers in the synthesis technique of benzimidazole and its derivatives increased. Researchers were inspired by these early findings to investigate

the nucleus of benzimidazole for a variety of purposes. Because of its presence in a wide range of biologically active compounds, including antiparasitics, antimicrobials, antivirals, antifungals, anticonvulsants, antihypertension medications and analgesics, anti-inflammatory drugs, anticancer drugs and anticoagulant agents, benzimidazole has emerged as an important heterocyclic system over the course of many years of research(Fei and Zhou, 2013; Wang et al., 2015).

Many drugs with diverse therapeutic lines have been developed as a result of substituent changes around the core structure, including albendazole, mebendazole, and thiabendazole as antihelmintics; enviradine as antiviral; carbendazim as fungicidal; omeprazole, lansoprazole, and pantoprazole as proton pump inhibitors; candesartan cilexitil and telmisartan as antihypertensives, and astemizole as antihistaminic agent(Alaqeel, 2017; Bansal and Silakari, 2012). Medical chemists have been motivated to synthesize various new therapeutic compounds containing the benzimidazole moiety due to the excellent therapeutic potential of benzimidazole-related therapeutics(S. Khan et al., 2021; Khan et al., 2020; Mayura et al., 2019; Morais et al., 2017; Shntaif et al., 2021; Siddiqui et al., 2021). Recently, **Khan et al.** synthesized and analyzed pyrimidine-linked benzimidazole hybrids and identified their antibacterial and antifungal activity *in vitro*, as well as their capacity to inhibit the main protease and spike glycoprotein of SARS-CoV-2(S. Khan et al., 2021). Several review papers have been published that highlight the role of the benzimidazole nucleus in biological activity, such as anticancer, analgesic, antiinflammatory, antibacterial, antiviral, antitubercular, antiulcer, antihypertensive, and antidiabetic properties(Morais et al., 2017).

After knowing the importance of benzimidazoles in various diseases, in present work, we aimed at preparing some 2-(2-phenyl-1*H*-benzo[*d*]imidazol-1-yl) acetic acid derivatives as potential angiotensin-II receptor inhibitors. The designed derivatives were subjected for the calculations of Lipinski rule, Veber's rule, ADME analysis, drug-likeness properties and molecular docking. The derivatives which successfully passed all the criteria and found potent through *in silico* screening were preceded for the wet lab synthesis, *in vitro*, and *in vivo* biological evaluation.

2. Material and Methods

2.1 Selection of Parent Nucleus and Designing of Derivatives

2-(2-phenyl-1*H*-benzo[*d*]imidazol-1-yl) acetic acid was selected as parent nucleus to construct the novel derivatives. The structures of designed derivatives and parent nucleus are illustrated in Fig. 1.

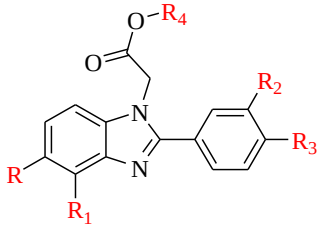

2-(2-phenyl-1*H*-benzo[*d*]imidazol-1-yl)acetic acid derivatives

Fig. 1. The parent nucleus

2.2 Pharmacokinetics predictions of designed derivatives

Utilizing molinspiration and SwissADME servers, Lipinski rule of five and pharmacokinetic features of developed derivatives were investigated(Daina et al., 2017; Kim et al., 2021). An *in silico* toxicity prediction of designed derivatives has been made using ProTox-II, a webserver that is freely available(http://tox.charite.de/protox_II)(Banerjee et al., 2018).

2.3 Molecular docking studies

In order to further optimization, the derivatives were subjected for binding affinity studies with human angiotensin receptor. The Autodock vina 1.1.2 with PyRx Virtual Screening Tool 0.8 software of the Chimera version 1.10.2(Dallakyan and Olson, 2015) and the Biovia Discovery studio was used to perform molecular docking(Miyata, 2015). The structures of 2-(2-phenyl-1*H*-benzo[*d*]imidazol-1-yl)acetic acid derivatives and native ligand were drawn using ChemDraw Ultra 8.0 version and saved in mol file format. The energy minimization was executed by Universal Force Field (UFF) in PyRx software(Rappé et al., 1992). The crystal structure of the XFEL structure of human angiotensin receptor (PDB ID: 4YAY) was obtained from the RCSB Protein

Data Bank (https://www.rcsb.org/). The 3D ribbon view of angiotensin receptor with native ligand is illustrated in Fig. 2. The binding mode and binding affinity of native ligand was used to validate the results of designed derivatives. With an exhaustiveness value of 8, the three-dimensional grid box (size_x = 49.1531A°, size_y = 38.5281A°, size_z = 42.6578A°) was modified for molecular docking simulations. The complete molecular docking approach was carried out in accordance with the methods outlined by S. L. Khan *et al.*(Chaudhari et al., 2020; Khan, Sharuk L; Siddiui, 2020; S. Khan et al., 2021; Khan et al., 2020; S. L. Khan et al., 2021; Siddiqui et al., 2021).

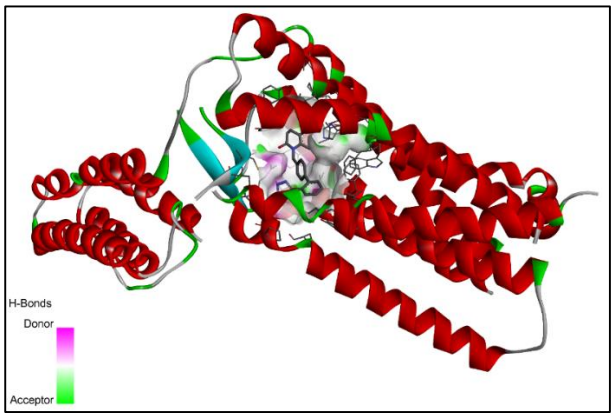

Fig. 2. The 3D ribbon view of angiotensin receptor with native ligand

2.4 Wet Lab Synthesis of Selected Derivatives

All the chemicals of synthetic and analytical grades were purchased and procured from Lab Trading Chemicals, Auranagabad, Maharashtra, India. The procedure applied for the synthesis of derivatives are given in the below section.

Step-I: 0.01 mole of substituted o-phenylenediamine and 0.01 mole of substituted aromatic aldehyde were added in round bottom flask of 250 mL. The mixture was kept for reflux on a water bath at 100 °C for 2 h. The reaction mixture was cooled and 10% sodium hydroxide solution was added slowly, with constant rotation of the flask, until the mixture is just alkaline to litmus. The synthesized crude benzimidazole was flittered by using the pump, washed with ice cold water, drained well and washed again with 25 ml of cold water. The product was recrystallized by dissolving in 40 mL of boiling water and 1 gm of decolorizing carbon and it was again stirred for 15 min. The product was filtered rapidly through a preheated Buchner funnel and a flask at the pump. The filtrate was cooled to about 10 °C, and then the benzimidazole was filtered off and washed with 25 ml of cold water and dried at 100 °C.

Step-II: 0.01 mole of benzimidazole intermediate and 0.01 mole of substituted aryl chloride was added in a round bottomed flask of 250 mL. The mixture was heated on a water bath at 100 °C for 2 h. The progress of the reaction was monitored by TLC using Toluene: Methanol (3:1) as solvent system and iodine vapor as a visualizing agent. The rests of procedure was employed as used for step-I. The obtained compounds were subjected for spectral analysis by FTIR, NMR, and Mass. The reaction scheme is illustrated in Fig. 3. The physicochemical data of synthesized compounds are tabulated in Table 1. The spectral interpretation of the compounds are given in the below section. The presence of number and nature of the hydrogen and carbon are determined by using ^{1}H-NMR and C^{13}-NMR technique using DMSO as a solvent and TMS as internal standard.

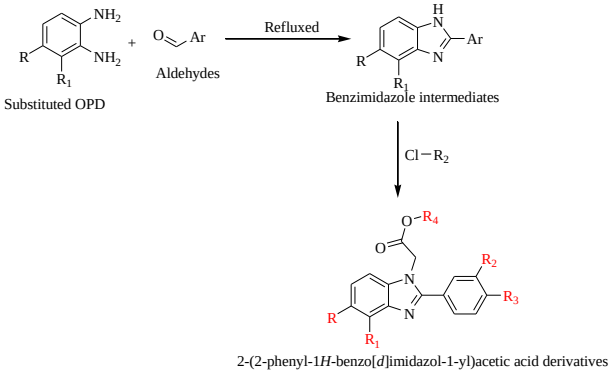

Fig. 3. The proposed reaction scheme for the synthesis of benzimidazole derivatives

Table 1. The physicochemical data of the synthesized compounds

Code	Molecular formula	Molecular Weight (gm/mol)	m.p. (^{0}C)	% Yield	Rf value	Elemental analysis		
						C	H	N
A_1	$C_{19}H_{20}N_2O_4$	340.37	168-172	0.58	0.58	67.05	5.92	8.23
A_6	$C_{20}H_{21}ClN_2O_2$	356.84	161-163	0.56	0.55	74.51	6.88	8.69
A_7	$C_{17}H_{16}N_2O_4$	312.31	167-170	0.59	0.58	65.38	5.16	8.97
A_{11}	$C_{16}H_{12}Cl_2N_2O_3$	351.18	169-174	0.63	0.57	54.72	3.44	7.98
A_{12}	$C_{16}H_{14}N_2O_3$	282.29	176-178	0.59	0.56	68.07	5.00	9.92
A_{13}	$C_{16}H_{13}ClN_2O_2$	300.73	180-182	0.57	0.54	63.90	4.36	9.31
A_{14}	$C_{15}H_{10}ClN_3O_4$	331.71	190-193	0.68	0.53	54.31	3.04	12.67
A_{15}	$C_{15}H_9Cl_2N_3O_4$	366.15	186-189	0.57	0.57	49.20	2.48	11.18
A_{18}	$C_{16}H_{14}N_2O_5$	314.29	178-182	0.61	0.63	61.14	4.49	8.91

A_1: MS: (m/e): 340.37. FTIR (cm^{-1}):3245.28 (-NH str.); 3025.65 (Ar –CH str.); 2850.26 (-CH_3 str.); 1585.35 (-C=N str.); 1252.64 (-C-N str.). ^{1}H-NMR (ppm): 6.5-7.4 5H of Phenyl; 5.0 2H of –OH; 1.2-1.5 6H of –CH_3; 2.2 2H of –CH_2; 2.0-2.4 5H of –C_2H_5. ^{13}C NMR ($CHCl_3$-d_6 400 MHz) δ ppm: 12.7, 14.1, 17.8, 50.8, 61.00, 117.8, 121.5, 124.7, 125.3, 130.4, 147.8, 153.3, 166.3.

A_6: MS: (m/e): 356.84. FTIR (cm^{-1}): 3256.45 (-NH str.); 3015.24 (Ar –CH str.); 2865.34 (-CH_3 str.); 1578.34 (-C=N str.); 1265.35 (-C-N str.). ^{1}H-NMR (ppm): 7.0-7.4 5H of Phenyl; 1.2-1.4 9H of –CH_3; 2.0 2H of –CH_2; 1.6-1.8 5H of –C_2H_5. ^{13}C NMR ($CHCl_3$-d_6 400 MHz) δ ppm: 10.1, 14.1, 40.3, 50.8, 61.00, 113.4, 114.8, 120.4, 124.5, 128.7, 132.3, 139.4, 149.4, 153.3, 166.3.

A_7: MS: (m/e): 312.31. FTIR (cm^{-1}): 3228.35 (-NH str.); 3026.34 (Ar –CH str.); 2865.34 (-CH_3 str.); 1575.64 (-C=N str.); 1225.65 (-C-N str.). ^{1}H-NMR (ppm): 6.6-7.2 6H of Phenyl; 5.0 2H of –OH; 1.0-1.4 3H of –CH_3; 2.0 2H of –CH_2; 1.8-2.0 3H of –OCH_3. ^{13}C NMR ($CHCl_3$-d_6 400 MHz) δ ppm: 19.2, 50.8, 51.00, 104.1, 109.0, 111.1, 112.4, 122.9, 130.8, 134.2, 138.2, 120.4, 122.9, 153.3, 159.9, 166.3.

A_{11}: MS: (m/e): 351.18. FTIR (cm^{-1}): 3228.26 (-NH str.); 3010.65 (Ar –CH str.); 2865.30 (-CH_3 str.); 1590.35 (-C=N str.); 1265.38 (-C-N str.). ^{1}H-NMR (ppm): 6.8-7.6 5H of Phenyl; 5.0 1H of –OH; 2.4 2H of –CH_2; 1.8-2.0 3H of –OCH_3. ^{13}C NMR ($CHCl_3$-d_6 400 MHz) δ ppm:

A_{12}: MS: (m/e): 282.29. FTIR (cm^{-1}): 3265.23 (-NH str.); 3026.14 (Ar –CH str.); 2845.34 (-CH_3 str.); 1586.47 (-C=N str.); 1250.36 (-C-N str.). ^{1}H-NMR (ppm): 6.8-7.2 6H of Phenyl; 10.45 1H of –COOH; 5.0 1H of –OH; 2.4 2H of –CH_2. ^{13}C NMR ($CHCl_3$-d_6 400 MHz) δ ppm: 14.1, 50.8, 61.00, 107.9, 111.4, 121.4, 124.5, 128.7, 125.3, 130.4, 133.4, 147.8, 153.3, 166.3.

A_{13}: MS: (m/e): 300.73. FTIR (cm^{-1}): 3285.48 (-NH str.); 3015.45 (Ar –CH str.); 2864.26 (-CH_3 str.); 1590.35 (-C=N str.); 1265.32 (-C-N str.). ^{1}H-NMR (ppm): 6.8-7.2 6H of Phenyl; 10.45 1H of –COOH; 2.0 2H of –CH_2; 1.0 3H of –CH_3. ^{13}C NMR ($CHCl_3$-d_6 400 MHz) δ ppm: 19.2, 50.8, 51.00, 104.1, 109.0, 111.1, 112.4, 122.9, 130.8, 134.2, 138.2, 120.4, 122.9, 153.3, 159.9, 166.3.

A_{14}: MS: (m/e): 331.71. FTIR (cm^{-1}): 3245.28 (-NH str.); 3025.65 (Ar –CH str.); 2850.26 (-CH_3 str.); 1585.35 (-C=N str.); 1252.64 (-C-N str.). ^{1}H-NMR (ppm): 6.8-7.2 6H of Phenyl; 10.3 1H of –COOH; 2.0 2H of –CH_2. ^{13}C NMR ($CHCl_3$-d_6 400 MHz) δ ppm: 14.1, 50.8, 61.00, 107.9, 111.4, 121.4, 124.5, 128.7, 125.3, 130.4, 133.4, 147.8, 153.3, 166.3.

A_{15}: MS: (m/e): 366.15. FTIR (cm^{-1}): 3228.26 (-NH str.); 3010.65 (Ar –CH str.); 2865.30 (-CH_3 str.); 1590.35 (-C=N str.); 1265.38 (-C-N str.). ^{1}H-NMR (ppm): 6.6-7.0 6H of Phenyl; 10.45 1H of –COOH; 2.25 2H of –CH_2. ^{13}C NMR ($CHCl_3$-d_6 400 MHz) δ ppm: 19.2, 50.8, 51.00, 104.1, 109.0, 111.1, 112.4, 122.9, 130.8, 134.2, 138.2, 120.4, 122.9, 153.3, 159.9, 166.3.

A_{18}: MS: (m/e): 314.29. FTIR (cm^{-1}): 3285.65 (-NH str.); 3026.34 (Ar –CH str.); 2865.34 (-CH_3 str.); 1562.35 (-C=N str.); 1245.65 (-C-N str.). ^{1}H-NMR (ppm): 6.3-7.2 6H of Phenyl; 10.35 1H of –COOH; 5.0 2H of –OH; 2.25 2H of –CH_2; 1.15

3H of $-CH_3$. ^{13}C NMR ($CHCl_3$-d_6 400 MHz) δ ppm: 19.2, 50.8, 51.00, 104.1, 109.0, 111.1, 112.4, 122.9, 130.8, 134.2, 138.2, 120.4, 122.9, 153.3, 159.9, 166.3.

2.5 *In vitro* ACE enzyme assay

ACE inhibitor activity was determined using Cushman and Cheung method with some modifications. Substrate Hippuryl-L-histidyl-L-Leucine (HHL) and ACE were purchased from Sigma Aldrich and were dissolved in sodium borate buffer pH 8.3 containing 0.5 M NaCl. In each assay, as 40µl sample solution was added with 120 µl of 8.3 mM HHL and pre-incubated for 5 minutes at 37 ºC. The mixture was added with 40 µl of 25 mU/ml ACE and incubated for 30 minutes at 37 ºC. The reaction was terminated by adding 100 µl of 1 M HCl solution. Sodium borate buffer was added until the final volume of the mixture was 450 µl. Hippuric acid as a reaction product was extracted using 1 ml ethyl acetate and was centrifuged for 10 minutes at 3500 rpm. Ethyl acetate was evaporated at 95 ºC and the residue was dissolved in 1 mL of distilled water, then the absorbance was measured at 228 nm. The absorbance was used to estimate ACE inhibitor activity. The activity of each sample was measured in triplicate. To correct the interference compounds of the sample that can be extracted by ethyl acetate and had absorbance at the same wavelength, the absorbance of the sample was corrected with a blank sample. Control (C) was prepared as a sample, but by replacing the sample with sodium borate buffer. Blank reaction (B) was prepared by adding HCl after adding an ACE and replaced the sample with a buffer solution. Blank sample (D) was prepared by the same manner as blank reaction, but the sample was not replaced with buffer solution. Captopril was used as a positive control at concentration 2µg/mL. ACE inhibitor activity was expressed in percent inhibition; it was calculated using the following equation:

$$\text{ACE inhibitor activity (\%)} = [(C-B)-(A-D)]/(C-B)*100$$

Where, A, absorbance of sample; B, absorbance of blank reaction; C, absorbance of control; D, absorbance of blank sample.

2.6 *In vivo* Antihypertensive Activity using Tail Cuff Method

Drugs and Chemicals

Deoxycorticosterone acetate (DOCA) salt, carboxy methyl cellulose (CMC), prazosin, and all the other required chemicals of analytical grade were purchased and procured from Lab Trading Laboratory, Aurangabad, Maharashtra, India.

Animals and Ethical Approvals

Healthy Wistar rats of either sexes weighing 180 to 250 g were used in this study. They were kept in regular settings, with a temperature of 25^0C and a relative humidity of 45 to 55 percent. They were given a conventional pellet feed and free access to water *ad libitum*. In line with the Committee for the Purposes of Control and Supervision of Experiments on Animals' (CPCSEA) requirements all of the animals were observed and cared for in accordance with their needs. The animals were kept in polypropylene cages, and all procedures on them were carried out in an aseptic environment. With the approval of the Institutional Animal Ethics Committee (IAEC), the study's procedures were implemented (approval number CPCSEA/IAEC/JLS/16/07/21/36).

Induction of Hypertension and Grouping

One day prior to the experiment the animals were divided into seven different groups each containing six animals. Among the seven groups, one group served as a normal control. Hypertension was induced in other six groups with twice weekly administration of DOCA salt (20 mg/kg s.c) for 4 weeks. The alterations in the BP were recorded every week by rodent noninvasive blood pressure (tail cuff method) system. Hypertension was induced in 4 weeks, and when BP reached >140 mmHg, each group was assigned a specific treatment for 7 days in the 5th week. The detailed grouping of the animals is tabulated in Table 2. The hypertensive control group was treated with the vehicle that is, CMC. At the end of the 5th week again the BP was measured noninvasively to monitor the BP change in response to the test drug.

Table 2. The detailed grouping of the animals

Group name	Treatment
Group-I	Normal control
Group-II	Hypertensive control
Group-III	Standard (Prazosin 1mg/kg)
Group-IV	Sample-I (compound A1, 25mg/kg)
Group-V	Sample-I (compound A1, 50mg/kg)
Group-VI	Sample-II (compound A11, 25mg/kg)
Group-VII	Sample-II (compound A11, 50mg/kg)

After administration of various doses of the compounds (sample-I & II), blood pressure and heart rate of each of these groups were determined from the tails of rats using non-invasive blood pressure (NIBP) measuring apparatus (IN125, AD Instruments, Sydney, Australia). Each rat was placed in NIBP restrainer and appropriate cuff with sensor was then mounted on its tail and warmed to about 33 – 35 °C. The tail cuff (MLT 125/R) was inflated to a pressure well above the expected systolic blood pressure, i.e., 200 mm Hg, and slowly released during which the pulses were recorded by using Power Lab data acquisition system and computer running Lab Chart 5.0 software (Ad Instruments, Sydney, Australia). Systolic blood pressure (SBP), Mean blood pressure (MBP) and heart rate were measured directly using pulse tracing while diastolic blood pressure (DBP) was calculated from SBP and MBP as in below equation(Alamgeer et al., 2013; Bilanda et al., 2019; Ishii et al., 1996; Raveendran et al., 2014; Takeyama et al., 1985).

$$DBP = \frac{3MBP - SBP}{2}$$

The three parameters measured using a noninvasive method include systolic BP, diastolic BP, and heart rate.

3. Results

Pharmacokinetic features are crucial in drug development because they allow researchers to evaluate the biological elements of potential medications. Lipinski's rule of five and Veber's rules were used to determine if the compounds were ideal for oral bioavailability (Table 3). To further understand their pharmacokinetics profiles and drug-likeness properties, all of the proposed compounds were investigated for their ADME characteristics (Table 4). The oral acute toxicity have been predicted along with LD_{50} (mg/kg), toxicity class, hepatotoxicity, carcinogenicity, immunotoxicity, mutagenicity, and cytotoxicity (Table 5).

Table 3. Calculations of Lipinski's rule of five and Veber's rule for the designed derivatives

Compound Codes	Lipinski rule of five					Veber's rule	
	Log P	Mol. Wt.	HBA	HBD	Violations	Total polar surface area (Å^2)	No. of rotatable bonds
NL	4.05	438.52	5	1	0	87.66	6
A1	2.98	340.37	5	2	0	84.58	5
A2	3.25	381.21	5	2	0	84.58	5
A3	3.77	365.21	4	1	0	64.35	5
A4	-1.54	342.33	6	2	0	114.01	6
A5	3.98	371.86	3	0	0	47.36	6
A6	4.56	356.85	3	0	0	44.12	5
A7	2.33	312.32	5	2	0	84.58	4
A8	1.96	328.32	6	2	0	93.81	5

A9	2.88	346.77	5	2	0	84.58	4
A10	4.3	369.63	3	0	0	44.12	4
A11	3.41	351.18	4	1	0	64.35	4
A12	2.3	282.29	4	2	0	75.35	3
A13	3.24	300.74	3	1	0	55.12	3
A14	-1.76	332.72	5	2	0	104.78	4
A15	-1.93	367.16	5	2	0	104.78	4
A16	-2.47	330.27	7	4	0	145.24	4
A17	-7.24	344.28	7	3	0	154.44	5
A18	1.59	314.29	6	3	0	104.81	4
A19	4.29	369.63	3	1	0	55.12	3
A20	3.77	335.18	3	1	0	55.12	3
A21	4.29	369.63	3	1	0	55.12	3
A22	2.88	316.74	4	2	0	75.35	3

Where: Mol. Wt., molecular weight; HBA, hydrogen bond acceptors; HBD, hydrogen bond donors

Table 4. The pharmacokinetics and drug-likeness properties of developed compounds

Compound codes	Pharmacokinetics									Drug-likeness			
	GI abs.	BBB pen.	P-gp sub.	CYP1A2	CYP2C19	CYP2C9	CYP2D6	CYP3A4	Log K_p (skin permeation, cm/s)	Ghose	Egan	Muegge	Bioavailability Score
				inhibitors									
NL	High	No	Yes	No	Yes	Yes	Yes	Yes	-5.96	1	0	0	0.56
A1	High	No	No	Yes	No	Yes	Yes	No	-5.88	0	0	0	0.55
A2	High	No	No	Yes	Yes	Yes	Yes	No	-5.76	0	0	0	0.55
A3	High	Yes	No	Yes	Yes	Yes	No	No	-5.41	0	0	0	0.55
A4	High	No	Yes	No	No	No	No	No	-6.61	0	0	0	0.55
A5	High	Yes	No	Yes	Yes	Yes	Yes	Yes	-5.3	0	0	0	0.55
A6	High	Yes	No	Yes	Yes	Yes	No	No	-4.78	0	0	1	0.55
A7	High	No	No	Yes	No	No	No	No	-6.23	0	0	0	0.55
A8	High	No	No	Yes	No	No	No	No	-6.61	0	0	0	0.55
A9	High	No	No	Yes	No	Yes	No	No	-6	0	0	0	0.55
A10	High	Yes	No	Yes	Yes	Yes	No	No	-5	0	0	1	0.55
A11	High	Yes	No	Yes	Yes	Yes	No	No	-5.59	0	0	0	0.55
A12	High	Yes	No	Yes	No	No	No	No	-6.03	0	0	0	0.56
A13	High	Yes	No	Yes	Yes	Yes	No	No	-5.44	0	0	0	0.85
A14	High	No	Yes	No	No	No	No	No	-6.35	0	0	0	0.56
A15	High	No	Yes	No	No	No	No	No	-6.11	0	0	0	0.56
A16	Low	No	Yes	No	No	No	No	No	-7.29	0	1	0	0.56
A17	Low	No	Yes	No	No	No	No	No	-7.31	0	1	1	0.11
A18	High	No	Yes	No	No	No	No	No	-6.75	0	0	0	0.56
A19	High	Yes	No	Yes	Yes	Yes	No	No	-4.98	0	0	1	0.85
A20	High	Yes	No	Yes	Yes	Yes	No	No	-5.21	0	0	0	0.85
A21	High	Yes	No	Yes	Yes	Yes	No	No	-4.98	0	0	1	0.85
A22	High	Yes	No	Yes	No	No	No	No	-5.8	0	0	0	0.56

Where: NL, Native ligand; GI abs., gastrointestinal absorption; BBB pen., blood brain barrier penetration; P-gp sub., p-glycoprotein substrate substrate.

Table 5. The predicted acute toxicity of developed molecules

Compound codes	Parameters							
	LD_{50} (mg/kg)	Toxicity class	Prediction accuracy (%)	Hepatotoxicity (Probability)	Carcinogenicity (Probability)	Immunotoxicity (Probability)	Mutagenicity (Probability)	Cytotoxicity (Probability)
NL	2100	5	67.38	A (0.60)	A (0.52)	I (0.96)	A (0.51)	I (0.62)
A1	1600	4	67.38	I (0.73)	I (0.56)	I (0.73)	I (0.64)	I (0.57)
A2	1600	4	67.38	I (0.61)	I (0.60)	I (0.59)	I (0.69)	I (0.55)
A3	1600	4	67.38	I (0.62)	I (0.59)	I (0.72)	I (0.68)	I (0.56)
A4	800	4	67.38	I (0.66)	I (0.55)	I (0.58)	I (0.67)	I (0.55)
A5	1000	4	67.38	I (0.66)	I (0.55)	I (0.58)	I (0.67)	I (0.55)
A6	1000	4	67.38	I (0.74)	I (0.62)	I (0.87)	I (0.70)	I (0.63)
A7	1600	4	67.38	I (0.65)	I (0.57)	A (0.87)	I (0.63)	I (0.55)
A8	1600	4	67.38	I (0.67)	I (0.61)	A (0.79)	I (0.64)	I (0.51)
A9	1600	4	67.38	I (0.52)	I (0.63)	A (0.67)	I (0.74)	I (0.52)
A10	1000	4	67.38	I (0.66)	I (0.64)	I (0.83)	I (0.75)	I (0.62)
A11	1600	4	67.38	I (0.50)	I (0.62)	A (0.68)	I (0.72)	I (0.53)
A12	1500	4	67.38	I (0.67)	I (0.57)	A (0.99)	I (0.65)	I (0.61)
A13	800	4	67.38	I (0.63)	I (0.65)	I (0.98)	I (0.79)	I (0.66)
A14	1500	4	67.38	I (0.50)	I (0.62)	A (0.68)	I (0.72)	I (0.53)
A15	1000	4	67.38	I (0.63)	I (0.65)	I (0.98)	I (0.79)	I (0.66)
A16	2000	4	67.38	I (0.66)	I (0.64)	I (0.83)	I (0.75)	I (0.62)
A17	2872	5	67.38	I (0.63)	I (0.57)	A (0.98)	I (0.63)	I (0.57)
A18	1000	4	67.38	I (0.63)	I (0.57)	A (0.98)	I (0.63)	I (0.57)
A19	22	2	67.38	I (0.63)	I (0.65)	A (0.77)	I (0.79)	I (0.66)
A20	6	2	67.38	I (0.63)	I (0.65)	I (0.85)	I (0.79)	I (0.66)
A21	22	2	67.38	I (0.63)	I (0.65)	A (0.77)	I (0.79)	I (0.66)
A22	800	4	67.38	I (0.50)	I (0.60)	A (0.92)	I (0.73)	I (0.55)

Where: I, Inactive; A, Active

From the initial screening through Lipinski rule, Veber's rule, ADME calculations, and drug-likeness properties, molecules **A16, A17, A19, A20** and **A21** violated the most drug-likeness characteristics. Therefore only remaining molecules were subjected for molecular docking studies. Many of the molecules selected for docking had exhibited potent interactions and binding energy than native ligand with the target. The molecules' 2D and 3D docking postures (most potent) are represented in Fig. 4.

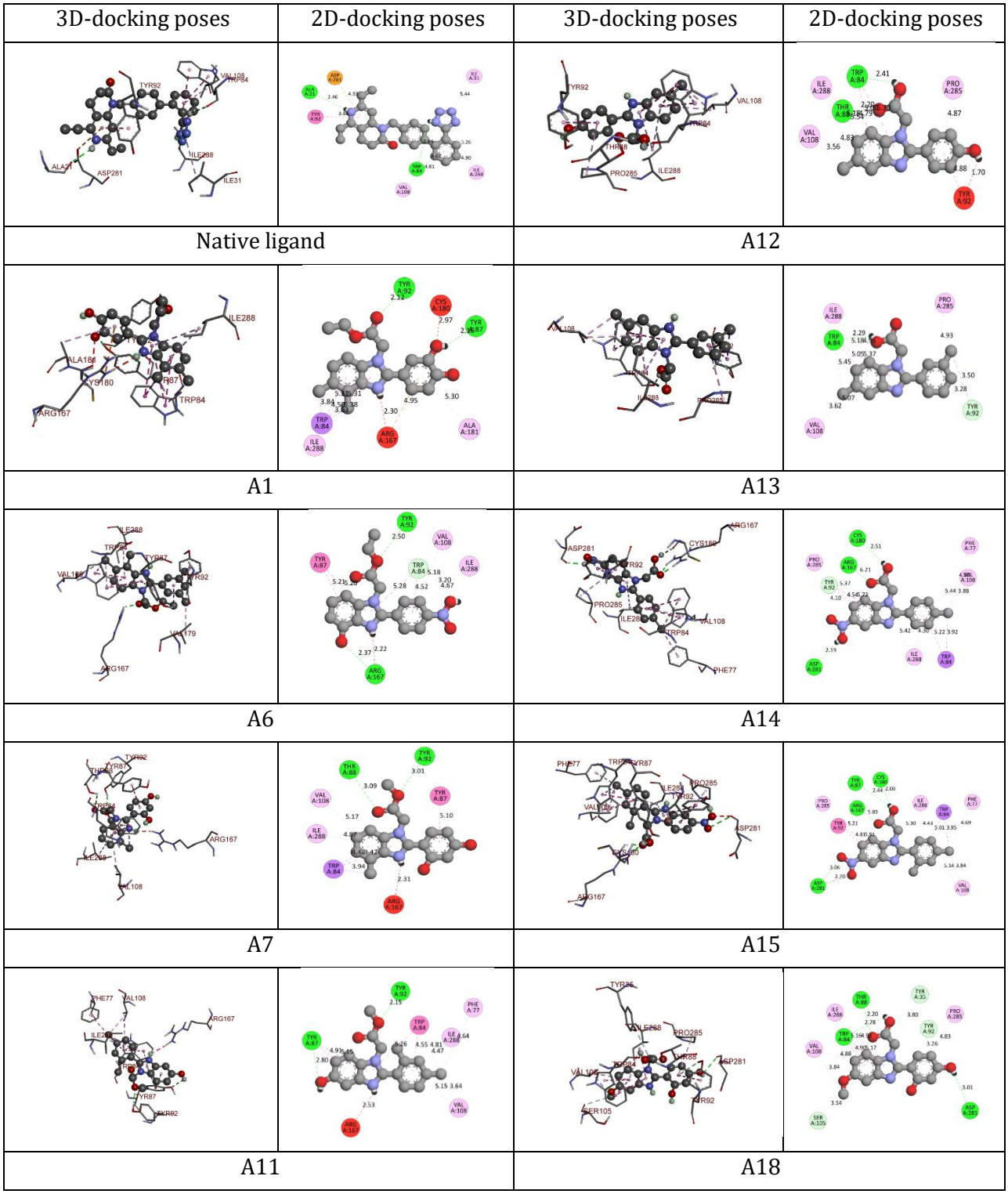

Fig. 4. The binding poses and 2D interactions of native ligand and most potent derivatives

In vitro ACE inhibitor Assay

The *in vitro* angiotensin enzyme assay was performed on all of the synthesized compounds and the results are tabulated in Table 6.

Table 6. *In vitro* ACE inhibitor activity of synthesized compounds

Compound	Conc. (µg/mL)	%ACE Inhibition (Mean ± SD)	IC_{50} (µg/mL)
A1	2	61.12 ± 0.16*	0.52
A6	2	60.28 ± 0.16*	0.74
A7	2	66.20 ± 0.18*	0.81
A11	2	61.90 ± 0.32*	0.47
A12	2	60.35 ± 0.25*	0.89
A13	2	61.36± 0.18*	1.10
A14	2	60.64 ± 0.16*	0.67
A15	2	60.36 ± 0.24*	0.95
A18	2	63.47 ± 0.19*	0.67
Captopril	2	66.25 ± 0.13*	0.45

In vivo Antihypertensive Activity using Tail Cuff Method

From *in vitro* screening two most potent compound [A1 (sample-I), A11 (sample-II)] selected for the *in vivo* screening. The *in vivo* antihypertensive activity of the selected benzimidazole derivatives was determined by using Tail Cuff method in which the three parameters measured using a noninvasive method include systolic BP, diastolic BP, and heart rate and the data on the parameters are presented in Tables 7 and 9.

Table 7. Effect of compounds on systolic BP (mmHg) in DOCA induced hypertensive rats

Groups	0 week	1 week	2 week	3 week	4 week	5 week
Normal control	105.5±9.2	123.6±7.1	117.4±5.2	102.2±9.7	121.1±6.1	118.8±3.4
Hypertensive control	121.1±3.2	132.8±2.7	147.8±6.8	159.5±3.8	180.2±3.8[b]	164.7±7.6
Standard (Prazosin 1mg/kg)	109.1±5.2	112.3±3.2	130.7±1.5	147.4±3.7	160.6±2.5[b]	103.5±7.3[a]
Sample-I (25mg/kg)	108.1±2.3	120.4±3.2	129.6±1.9	146.3±4.2	157.8±5.3[b]	121.5±9.8[a]
Sample-I (50mg/kg)	103.6±6.1	122.9±5.6	110.2±4.9	131.9±2.7	149.1±3.5[b]	120.8±11.4[a]
Sample-II (25mg/kg)	107.3±2.4	119.7±3.4	129.8±1.2	144.3±4.1	156.3±5.2[b]	120.1±9.9[a]
Sample-II (50mg/kg)	101.3±6.4	121.5±5.7	109.3±4.7	130.2±4.3	148.2±3.5[b]	118.7±12.6[a]

Values are mean±SEM. n=6 in each group. [a]P<0.05 versus DOCA 4 weeks group, [b]P<0.05 versus baseline value. Two-way repeated measures ANOVA followed by Bonferroni post-hoc test. DOCA: Deoxycorticosterone acetate salt (20 mg/kg s.c), BP: Blood pressure, SEM: Standard error of the mean

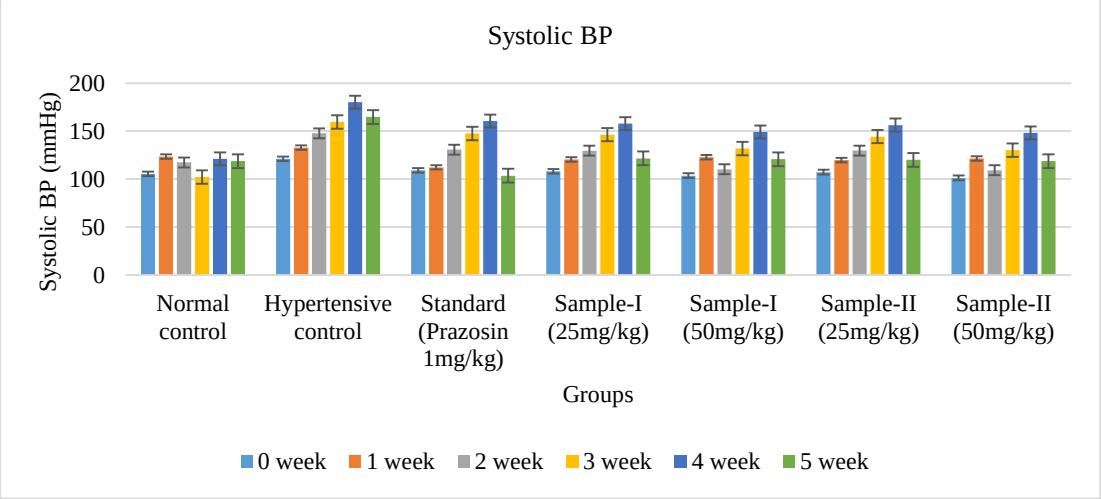

Fig. 5. Effect of compounds on systolic BP (mmHg) in DOCA induced hypertensive rats

Table 8. Effect of compounds on diastolic BP (mmHg) in DOCA induced hypertensive rats

Groups	0 week	1 week	2 week	3 week	4 week	5 week
Normal control	53.8±4.9	59.1±5.8	58.6±3.5	54.6±2.5	69.6±9.1	64.9±2.9
Hypertensive control	61.1±1.8	53.7±5.7	64.8±5.8	62.4±6.1	78.9±6.2[b]	82.1±3.8
Standard (Prazosin 1mg/kg)	54.2±3.8	57.2±1.4	61.7±2.8	69.4±1.0	80.4±2.1[b]	52.2±3.9[a]
Sample-I (25mg/kg)	56.2±3.2	61.2±1.5	67.9±2.6	71.5±1.1	82.3±2.3[b]	61.5±3.6[a]
Sample-I (50mg/kg)	55.2±3.7	58.2±1.2	62.7±2.8	70.4±1.5	81.4±1.5[b]	58.2±3.2[a]
Sample-II (25mg/kg)	56.6±3.5	61.1±1.7	68.4±2.8	72.5±1.4	83.2±2.6[b]	61.7±4.6[a]
Sample-II (50mg/kg)	53.9±3.2	57.2±2.1	62.1±2.1	69.9±1.3	80.2±1.9[b]	54.6±3.0[a]

Values are mean±SEM. n=6 in each group. [a]P<0.05 versus DOCA 4 weeks group, [b]P<0.05 versus baseline value. Two-way repeated measures ANOVA followed by Bonferroni post-hoc test. DOCA: Deoxycorticosterone acetate salt (20 mg/kg s.c), BP: Blood pressure, SEM: Standard error of the mean

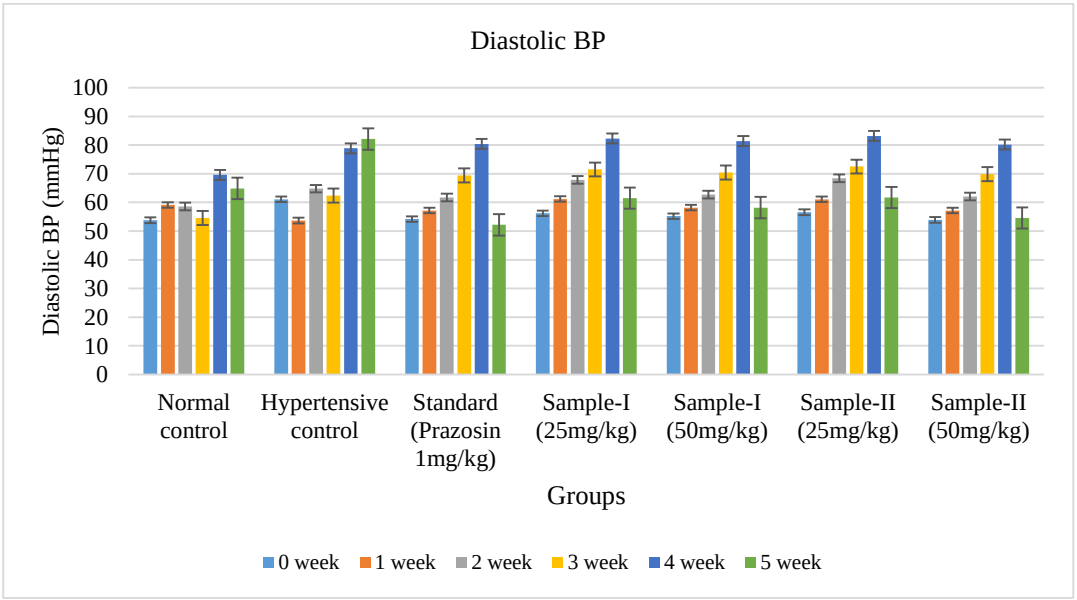

Fig 6. Effect of compounds on diastolic BP (mmHg) in DOCA induced hypertensive rats

Table 9. Effect of compounds on heart rate (beats/min) in DOCA induced hypertensive rats

Groups	0 week	1 week	2 week	3 week	4 week	5 week
Normal control	340.7±21.8	338.1±54.1	368.5±43.2	305.5±34.2	414±38.9	441.7±32.4
Hypertensive control	342.5±41.3	252±52.5	267.4±41.3	335.5±63.7	399.3±79.2	387.9±81.7
Standard (Prazosin 1mg/kg)	303.5±32.3	299.9±23.9	304±42.4	298.5±41.4	387.5±45.2	303.2±46.2
Sample-I (25mg/kg)	337.1±62.2	252±46.62	289±42.5	327.6±47.2	288.8±37.2	308.2±8.4
Sample-I (50mg/kg)	330.1±61.7	249±43.62	281±47.5	322.4±41.4	283.3±32.1	303.2±8.3
Sample-II (25mg/kg)	335.1±63.2	250±45.62	284±42.5	322.6±44.2	285.9±32.5	298.3±8.7
Sample-II (50mg/kg)	312.1±51.3	242±42.63	280±39.1	318.6±34.2	278.2±22.8	290.2±9.5

Values are mean±SEM. n=6 in each group. Two-way repeated measures ANOVA followed by Bonferroni *post-hoc* test. DOCA: Deoxycorticostrerone acetate salt (20 mg/kg s.c), BP: Blood pressure, SEM: Standard error of the mean

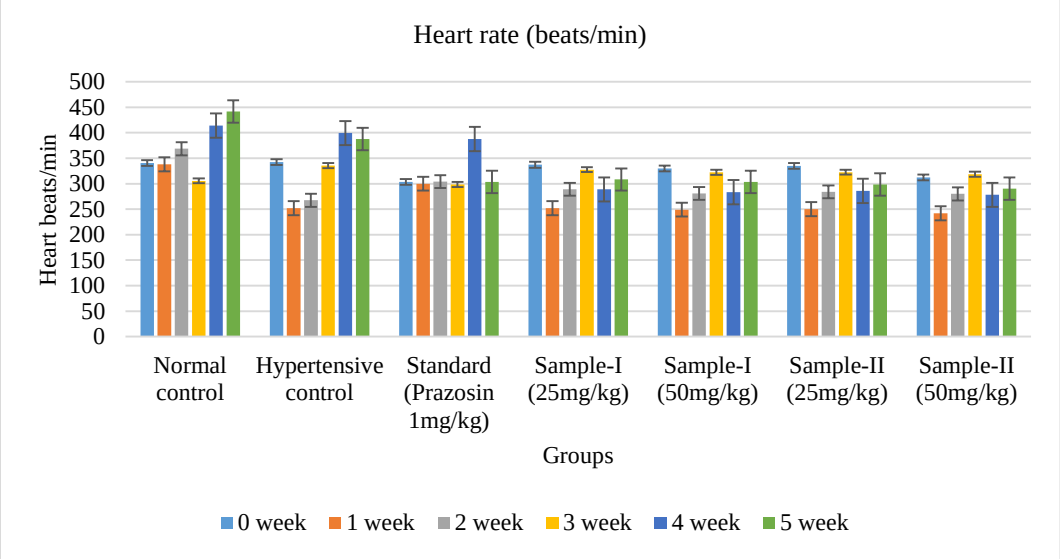

Fig 7. Effect of compounds on heart rate (beats/min) in DOCA induced hypertensive rats

4. Discussion

It is the primary goal of medication development to transform a therapeutic molecule into a dosage form that can be administered to patients. Pharmacological effects must occur at the site of action and be eradicated within an acceptable time period; this is preferable to once-a-day use. It is possible to make risk-based evaluations of a novel drug's safety by characterizing its absorption, distribution, metabolism, and excretion (ADME) features(Akhtar et al., 2017; Barret, 2018; Kamal et al., 2015). This helps to study and explain how pharmacokinetic processes occur. We have designed some 2-(2-phenyl-1*H*-benzo[*d*]imidazol-1-yl) acetic acid derivatives as potential human angiotensin receptor inhibitors through rational drug design approach. All the designed derivatives were subjected for ADMET analysis.

In accordance with Lipinski's and Veber's rule (Table 4), none of the molecule has violated the

Lipinski rule of five but few have violated the Veber's rule. The log P values of all the molecules found between -7.24 to 4.56 which indicate optimum lipophilicity. Lipophilicity is a significant feature of the molecule that affects how it works in the body(S. Khan et al., 2021). It is determined by the compound's Log P value, which measures the drug's permeability in the body to reach the target tissue(Krzywinski and Altman, 2013; Lipinski et al., 2012). The molecular weight of all the molecules was below 500 Da which indicates active better transport of the molecules through biological membrane. Fortunately, the Lipinski rule of 5 had not been compromised by the compounds, including native ligand (Khan et al., 2022; Shntaif et al., 2021). The total polar surface area (TPSA) and the number of rotatable bonds have been found to better discriminate between compounds that are orally active or not. According to Veber's rule, TPSA should be ≤ 140 and number of rotatable bonds should be ≤ 10. Compound A16 and A17 displayed TPSA value of 145.24 and 154.44 $Å^2$ which indicate these may not have optimum bioavailability.

In order to further optimize the compounds, pharmacokinetics and drug-likeness properties were calculated for each one. All the compounds excluding native ligand showed no penetration to the blood-brain barrier (BBB). The log *Kp* (skin penetration, cm/s) and bioavailability values of all the compounds were within acceptable limits. Few molecules do not meet all, two, or one of the Ghose, Egan, and Muegge requirements (Table 9). Many molecules found to be cytochrome enzyme inhibitors which indicates they will might be interfere with metabolism of other drugs. Molecules **A16** and **A17** exhibited low gastrointestinal (GI) absorption therefore these molecules were eliminated from further screening and did not subjected for molecular docking studies.

The binding affinities of all the docked derivatives have been compared with the binding mode of native ligand present in the crystal structure of human angiotensin enzyme (PDB ID: 4YAY). Native ligand exhibited binding affinity about -8 kcal/mol with enzyme and formed two conventional hydrogen bonds with Ala21 and Trp84. It has developed one electrostatic (Pi-anion) bond with Asp281. It exhibited hydrophobic (Pi-Pi stacked and Pi-alkyl) bonds with Tyr92, Trp84, Val108, Ile288, and Ile31. Compound **A1** displayed -8 kcal/mol binding affinity and also formed two conventional hydrogen bonds with Tyr87 and Tyr 92. It has formed only one electrostatic bond with Arg167 and many hydrophobic bonds with Trp84, ILe288 and Ala181. Compound **A6** showed -8.2 kcal/mol binding affinity and formed one conventional hydrogen bond with Arg167. It has developed many hydrophobic bonds with Trp84, Tyr92, Tyr92, Val179, Val108, and Ile288. Compound **A7** exhibited -8.4 kcal/mol docking score and formed two conventional hydrogen bonds with Thr88 and Tyr92. It has developed many hydrophobic interactions (Pi-sigma, Pi-Pi-stacked, Pi-Pi T-shaped) with Tyr92, Trp84, Tyr87, Val108, Ile288. Compound **A11** formed two conventional hydrogen bond with Tyr87, Tyr92 and exhibited -8.3 kcal/mol of binding energy. It has developed many hydrophobic interactions in same as compound A7 displayed. Compound **A12** exhibited -8.1 kcal/mol docking score and it has demonstrated interactions in a same way as compound **A7** and **A11** developed. Compound **A13** exhibited -8.6 kcal/mol docking score and formed one conventional hydrogen bond with Trp84 and Tyr92. It has developed many hydrophobic interactions (Pi-sigma, Pi-Pi-stacked, Pi-Pi T-pi-alkyl) with Tyr92, Trp84, Tyr87, Val108, and Ile288. Compound **A14** displayed -8.3 kcal/mol docking score and formed f our conventional hydrogen bonds with Cys180, Asp281, Arg167 and Tyr92. It has developed many hydrophobic interactions (Pi-sigma, Pi-Pi-stacked, alkyl, pi-alkyl) with Tyr92, Trp84, Tyr87, Val108, and Ile288. Compound **A15** displayed -8.6 kcal/mol docking score and formed four conventional hydrogen bonds with Cys180, Asp281, Arg167 and Tyr92. It has developed many hydrophobic interactions (Pi-sigma, Pi-Pi-stacked, alkyl, pi-alkyl) with Tyr92, Trp84, Tyr87, Val108, and Ile288. Compound **A18** displayed -8 kcal/mol docking score and formed three conventional hydrogen bonds with Asp281, Trp84 and Thr88, Carbon hydrogen bonds with Tyr35, Ser105 and Tyr92. It has developed many hydrophobic interactions (Pi-sigma, Pi-Pi-stacked, alkyl, pi-alkyl) with Tyr92, Trp84, Tyr87, Val108, and Ile288. Therefore from this investigation we have selected **A1, A6, A7, A11, A12, A13, A14, A15** and **A18** for the wet lab synthesis and biological evaluation.

The synthesized compounds have been confirmed by spectral analysis and subjected for *in vitro* enzyme assay followed by *in vivo* biological evaluation. The spectral interpretation of the compounds are already given in material method section. For *in vitro* assay, Captopril (approved ACE inhibitor) was used as standard to compare the compounds' inhibitory potential. Captopril displayed 66.25 ± 0.13% inhibition of the enzyme and exhibited 0.45 µg/mL IC_{50} value. The synthesized compounds demonstrated good inhibitory potential compared to Prazosin although did not exhibited more potency but can be considered active as angiotensin inhibitor. Out of screened derivatives as tabulated in Table 8, compounds A1, A11, A14, and A18 displayed 61.12 ± 0.16, 61.90 ± 0.32, 60.64 ± 0.16, and 63.47 ± 0.19% inhibition respectively. Moreover, compounds A1 and A11 showed most potent IC_{50} values of 0.52 and 0.47 µg/mL respectively. Therefore only these two molecules were subjected for *in vivo* antihypertensive activity.

Three parameters measured using a noninvasive method include systolic BP, diastolic BP, and heart rate. The results were compared with normal and hypertensive control and all the compounds displayed significant activity. The compounds which were under study showed dose dependent activity. In Prazosin treated groups it exhibited 109.1±5.2 mmHg systolic BP in first 0 week, which again increased to 112.3±3.2, 130.7±1.5, 147.4±3.7, and 160.6±2.5 mmHg in 1st, 2nd, 3rd, and 4th week which was again back to normal in 5th week i.e. 103.5±7.3 mmHg. Both the compound under study displayed same pattern of results in dose dependent. Sample-I (compound A1) at 50 mg/kg b.w. dose displayed 103.6±6.1 mmHg in 0 week which showed increase in systolic BP to 122.9±5.6, 110.2±4.9, 131.9±2.7, and 149.1±3.5 mmHg in 1st, 2nd, 3rd, and 4th week which was again back to normal in 5th week i.e. 120.8±11.4 mmHg. Compound A11 displayed more potent activity than compound A1, at dose of 50 mg/kg b.w. it showed 101.3±6.4 mmHg BP in 0 week which showed increase in systolic BP to 121.5±5.7, 109.3±4.7, 130.2±4.3, and 148.2±3.5 mmHg in 1st, 2nd, 3rd, and 4th week which was again back to normal in 5th week i.e. 118.7±12.6 mmHg.

All the treated animals were subjected for diastolic BP measurement and the results were significant when compared to the normal control group. In Prazosin treated group it displayed 54.2±3.8 mmHg diastolic BP which increased to 80.4±2.1 mmHg in 4th week of the treatment. It was observed that after the treatment of 5th week, it exhibited 52.2±3.9 mmHg diastolic BP which was significant when compared to the normal control. Compound A1 at 50 mg dose showed 55.2±3.7 mmHg BP which again showed increase in BP to 81.4±1.5 mmHg after 4th week but at the end of 5th week it exhibited 58.2±3.2 mmHg BP. In animals treated with compound A11, it displayed same pattern of the activity but after 5th week of treatment it displayed 54.6±3.0 mmHg BP which was significant when compared with the normal control group.

In normal control group, in 0 week rats displayed 340.7±21.8 heart rate which was increased to 441.7±32.4 beats/min in 5th week. In Prazosin treated group, in 0 week it showed 303.5±32.3beats/min heart rate which displayed increase in heart rate up to 4th week and showed normal at 5th week i.e. 303.2±46.2 beats/min. Compound A1 at 50 mg dose showed 330.1±61.7 beats/min heart rate which was 303.2±8.3 beats/min at 5th week which is same as that of Prazosin treated group. Compound A11 showed 290.2±9.5 beats/min heart rate after 5th week of treatment. From *in vivo* screening compound A11 displayed optimum control on systolic and diastolic BP as well as showed controlled heart rate (beats/min).

5. Conclusion

In present work, we aimed at preparing some 2-(2-phenyl-1*H*-benzo[*d*]imidazol-1-yl) acetic acid derivatives as potential angiotensin-II receptor inhibtors. The designed derivatives were subjected for the calculations of Lipinski rule, Veber's rule, ADME analysis, drug-likeness properties and molecular docking. The derivatives which successfully passed all the criteria and found potent through *in silico* screening were preceded for the wet lab synthesis, *in vitro*, and *in vivo* biological evaluation. In accordance with Lipinski's and Veber's rule, none of the molecule has violated the Lipinski rule of five but few have violated the Veber's rule. All the compounds excluding native ligand showed no penetration to the blood-brain barrier (BBB). The log *Kp* (skin

penetration, cm/s) and bioavailability values of all the compounds were within acceptable limits. Few molecules do not meet all, two, or one of the Ghose, Egan, and Muegge requirements. The synthesized compounds demonstrated good inhibitory potential compared to Captopril although did not exhibited more potency but can be considered active as angiotensin inhibitor. Out of screened derivatives, compounds A1 and A11 showed most potent IC_{50} values of 0.52 and 0.47 µg/mL respectively. From *in vivo* screening compound A11 displayed optimum control on systolic and diastolic BP as well as showed controlled heart rate (beats/min). From present study it was concluded that the compounds A1 and A11 have potent angiotensin receptor inhibitory potential and can be treated as potential lead nucleus to generate more potent antihypertensive agents.

Conflicts of Interest

Authors declared that there is no conflicts of interest exists

References

Akhtar, W., Khan, M.F., Verma, G., Shaquiquzzaman, M., Rizvi, M.A., Mehdi, S.H., Akhter, M., Alam, M.M., 2017. Therapeutic evolution of benzimidazole derivatives in the last quinquennial period. Eur. J. Med. Chem. 126, 705–753. https://doi.org/10.1016/j.ejmech.2016.12.010

Alamgeer, Akhtar, M.S., Jabeen, Q., Akram, M., Khan, H.U., Karim, S., Malik, M.N.H., Mushtaq, M.N., Salma, U., 2013. Antihypertensive activity of aqueous-methanol extract of Berberis orthobotrys Bien Ex Aitch in rats. Trop. J. Pharm. Res. 12, 393–399. https://doi.org/10.4314/tjpr.v12i3.18

Alaqeel, S.I., 2017. Synthetic approaches to benzimidazoles from o-phenylenediamine: A literature review. J. Saudi Chem. Soc. 21, 229–237. https://doi.org/10.1016/j.jscs.2016.08.001

Banerjee, P., Eckert, A.O., Schrey, A.K., Preissner, R., 2018. ProTox-II: A webserver for the prediction of toxicity of chemicals. Nucleic Acids Res. 46, W257–W263. https://doi.org/10.1093/nar/gky318

Bansal, Y., Silakari, O., 2012. The therapeutic journey of benzimidazoles: A review. Bioorganic Med. Chem. 20, 6208–6236. https://doi.org/10.1016/j.bmc.2012.09.013

Barot, K., Nikolova, S., Ivanov, I., Ghate, M., 2013. Novel Research Strategies of Benzimidazole Derivatives: A Review. Mini-Reviews Med. Chem. 13, 1421–1447. https://doi.org/10.2174/13895575113139990072

Barret, R., 2018. Lipinski's Rule of Five, in: Therapeutical Chemistry. pp. 97–100. https://doi.org/10.1016/b978-1-78548-288-5.50006-8

Bilanda, D.C., Tcheutchoua, Y.C., Djomeni Dzeufiet, P.D., Fokou, D.L.D., Fouda, Y.B., Dimo, T., Kamtchouing, P., 2019. Antihypertensive Activity of Leersia hexandra Sw. (Poaceae) Aqueous Extract on Ethanol-Induced Hypertension in Wistar Rat. Evidence-based Complement. Altern. Med. 2019. https://doi.org/10.1155/2019/2897867

Brink, N.G., Folkers, K., 1949. Vitamin B12. VI. 5,6-dimethylbenzimidazole, a degradation product of vitamin B12. J. Am. Chem. Soc. 71, 2951. https://doi.org/10.1021/ja01176a532

Chaudhari, R.N., Khan, S.L., Chaudhary, R.S., Jain, S.P., Siddiqui, F.A., 2020. B-Sitosterol: Isolation from Muntingia Calabura Linn Bark Extract, Structural Elucidation And Molecular Docking Studies As Potential Inhibitor of SARS-CoV-2 Mpro (COVID-19). Asian J. Pharm. Clin. Res. 13, 204–209. https://doi.org/10.22159/ajpcr.2020.v13i5.37909

Daina, A., Michielin, O., Zoete, V., 2017. SwissADME: A free web tool to evaluate pharmacokinetics, drug-likeness and medicinal chemistry friendliness of small molecules. Sci. Rep. 7. https://doi.org/10.1038/srep42717

Dallakyan, S., Olson, A.J., 2015. Small-molecule library screening by docking with PyRx. Methods Mol. Biol. 1263, 243–250. https://doi.org/10.1007/978-1-4939-2269-7_19

Fei, F., Zhou, Z., 2013. New substituted benzimidazole derivatives: A patent review (2010-2012). Expert Opin. Ther. Pat. 23, 1157–1179. https://doi.org/10.1517/13543776.2013.800857

Ishii, R., Tagawa, T., Ishida, T., Naruse, T., 1996. Antihypertensive effects of a new transdermal delivery system for clonidine in genetic and experimental hypertensive rats. Arzneimittel-Forschung/Drug Res. 46, 261–268.

Kamal, A., Shaik, A.B., Jain, N., Kishor, C., Nagabhushana, A., Supriya, B., Bharath Kumar, G., Chourasiya, S.S., Suresh, Y., Mishra, R.K., Addlagatta, A., 2015. Design and synthesis of pyrazole-oxindole conjugates targeting tubulin polymerization as new anticancer agents. Eur. J. Med. Chem. 92, 501–513. https://doi.org/10.1016/j.ejmech.2013.10.077

Khan, Sharuk L; Siddiui, F.A., 2020. Beta-Sitosterol: As Immunostimulant, Antioxidant and Inhibitor of SARS-CoV-2 Spike Glycoprotein. Arch. Pharmacol. Ther. 2. https://doi.org/10.33696/pharmacol.2.014

Khan, A., Unnisa, A., Sohel, M., Date, M., Panpaliya, N., Saboo, S.G., Siddiqui, F., Khan, S., 2022. Investigation of phytoconstituents of Enicostemma littorale as potential glucokinase activators through molecular docking for the treatment of type 2 diabetes mellitus. Silico Pharmacol. 10. https://doi.org/10.1007/s40203-021-00116-8

Khan, S., Kale, M., Siddiqui, F., Nema, N., 2021. Novel pyrimidine-benzimidazole hybrids with antibacterial and antifungal properties and potential inhibition of SARS-CoV-2 main protease and spike glycoprotein. Digit. Chinese Med. 4, 102–119. https://doi.org/10.1016/j.dcmed.2021.06.004

Khan, S.L., Siddiqui, F.A., Shaikh, M.S., Nema, N. V., Shaikh, A.A., 2021. Discovery of potential inhibitors of the receptor-binding domain (RBD) of pandemic disease-causing SARS-CoV-2 Spike Glycoprotein from Triphala through molecular docking. Curr. Chinese Chem. 01. https://doi.org/10.2174/2666001601666210322121802

Khan, S.L., Sonwane, G.M., Siddiqui, F.A., Jain, S.P., Kale, M.A., Borkar, V.S., 2020. Discovery of Naturally Occurring Flavonoids as Human Cytochrome P450 (CYP3A4) Inhibitors with the Aid of Computational Chemistry. Indo Glob. J. Pharm. Sci. 10, 58–69. https://doi.org/10.35652/igjps.2020.10409

Kim, S., Chen, J., Cheng, T., Gindulyte, A., He, J., He, S., Li, Q., Shoemaker, B.A., Thiessen, P.A., Yu, B., Zaslavsky, L., Zhang, J., Bolton, E.E., 2021. PubChem in 2021: New data content and improved web interfaces. Nucleic Acids Res. 49, D1388–D1395. https://doi.org/10.1093/nar/gkaa971

Krzywinski, M., Altman, N., 2013. Points of significance: Significance, P values and t-tests. Nat. Methods 10, 1041–1042. https://doi.org/10.1038/nmeth.2698

Lipinski, C.A., Lombardo, F., Dominy, B.W., Feeney, P.J., 2012. Experimental and computational approaches to estimate solubility and permeability in drug discovery and development settings. Adv. Drug Deliv. Rev. https://doi.org/10.1016/j.addr.2012.09.019

Mayura, K., Sharuk, K., Jyoti, H., 2019. Investigating Structural Requirements of Some Pyrimidine-linked Benzimidazole Derivatives as Anticancer Agents Against MCF-7 Cancerous Cell Line Through the use of 2D and 3D QSARs. Curr. Chem. Biol. 13, 232–249. https://doi.org/10.2174/2212796813666190207144407

Miyata, T., 2015. Discovery studio modeling environment. Ensemble 17, 98–104.

Morais, G.R., Palma, E., Marques, F., Gano, L., Oliveira, M.C., Abrunhosa, A., Miranda, H.V., Outeiro, T.F., Santos, I., Paulo, A., 2017. Synthesis and Biological Evaluation of Novel 2-Aryl Benzimidazoles as Chemotherapeutic Agents. J. Heterocycl. Chem. 54, 255–267. https://doi.org/10.1002/jhet.2575

Rappé, A.K., Casewit, C.J., Colwell, K.S., Goddard, W.A., Skiff, W.M., 1992. UFF, a Full Periodic Table Force Field for Molecular Mechanics and Molecular Dynamics Simulations. J. Am. Chem. Soc. 114, 10024–10035. https://doi.org/10.1021/ja00051a040

Raveendran, R., Parasuraman, S., Priyadharsini, R., 2014. Evaluation of the antihypertensive activity and alpha adrenergic receptor interaction of cleistanthins A and B. J. Basic Clin. Pharm. 5, 109. https://doi.org/10.4103/0976-0105.141950

Shntaif, A.H., Khan, S., Tapadiya, G., Chettupalli, A., Saboo, S., Shaikh, M.S., Siddiqui, F., Amara, R.R., 2021. Rational drug design, synthesis, and biological evaluation of novel N-(2-arylaminophenyl)-2,3-diphenylquinoxaline-6-sulfonamides as potential antimalarial, antifungal, and antibacterial agents. Digit. Chinese Med. 4, 290–304.

https://doi.org/10.1016/j.dcmed.2021.12.004

Siddiqui, F.A., Khan, S.L., Marathe, R.P., Nema, N. V., 2021. Design, Synthesis, and In Silico Studies of Novel N-(2-Aminophenyl)-2,3-Diphenylquinoxaline-6-Sulfonamide Derivatives Targeting Receptor- Binding Domain (RBD) of SARS-CoV-2 Spike Glycoprotein and their Evaluation as Antimicrobial and Antimalarial Agents. Lett. Drug Des. Discov. 18, 915–931. https://doi.org/10.2174/1570180818666210427095203

Takeyama, K., Minato, H., Fukuya, F., Kawahara, S., Hosoki, K., Kadokawa, T., 1985. Antihypertensive activity of alacepril, an orally active angiotensin converting enzyme inhibitor, in renal hypertensive rats and dogs. Arzneimittel-Forschung/Drug Res. 35, 1502–1507.

Wang, M., Han, X., Zhou, Z., 2015. New substituted benzimidazole derivatives: A patent review (2013-2014). Expert Opin. Ther. Pat. 25, 595–612. https://doi.org/10.1517/13543776.2015.1015987

Woolley, D.W., 1944. Some Biological Effects Produced By Benzimidazole and Their Reversal By Purines. J. Biol. Chem. 152, 225–232. https://doi.org/10.1016/s0021-9258(18)72045-0